Evaluation of High-cycle Fatigue Life of Aluminum Cast Alloy from Meso-level Consideration

Hiroshi NOGUCHI [1] **and Tatsujiro MIYAZAKI** [2]

[1]Department of Mechanical Science and Engineering, Faculty of Engneering,
Kyushu University, 6-10-1 Hakozaki, Fukuoka 812-8581, JAPAN.
[2]Graduate School of Engneering, Kyushu University,
6-10-1 Hakozaki, Fukuoka 812-8581, JAPAN.

ABSTRACT

In this paper, a growth rate law of a small crack under a large scale yielding is proposed for a generic metal material. A method is also proposed for considering the size distribution of spheroidal defects which interest with the specimen surface. Both methods are used to predict the high-cycle fatigue life with the large scatter due to the presence of defects. Moreover, rotating bending fatigue tests are carried out on Aluminum Cast Alloy with eutectic Si, Fe compounds and porosities. The present method for predicting fatigue life reliability from the meso-level consideration is examined and confirmed by comparing the predicted fatigue life distribution.

KEYWORDS

Metal Fatigue, Aluminum Cast Alloy, Fatigue Life, Fatigue Crack Growth, Statistics, Defect, Porosity, Recycle

INTRODUCTION

From a necessity of light transportation machine with a high specific strength, Aluminum Cast Alloy has been used in the engine and so on. 80% of material fracture is due to the fatigue. Therefore it is important to evaluate the fatigue characteristics as mechanical properties for machine designs. Moreover the results are useful for the improvement of reliability and alloy design. In researches on aluminum cast alloy, although many researches especially on shape and quantity of eutectic Si have been carried out [1-6], there are few researches on the effect of Fe introduced during the recycling process [2,3]. Fe forms a coarse needle shaped metal compound, and the compound decreases the flow of the melts and the mechanical properties. In order to decrease the bad effect of Fe, transition metals (Mn,Cr,Be and so on) are added to the aluminum cast alloy to improve the fracture toughness and breaking elongation by changing the Fe-compound's structure from a needle type to a Chinese script type [8-11]. The changing ratio depends on the composition ratio of the transition metal to Fe [12] and amount of an improving element Sr [13,14]. It is necessary to evaluate the effect the various Fe-compounds on the fatigue characteristics simply and quickly.

As afore mentioned, although it is necessary for practical use of new materials to evaluate the fatigue characteristics, a traditional macro-scale materials testing is useless because of the required long testing time. In order to overcome the problem, a new evaluation system for fatigue characteristics is constructed in this paper from meso-level considerations. Then it becomes possible to evaluate the fatigue characteristics of practical structures rapidly and to point out the direction of the material design reasonably.

PREDICTION OF HIGH CYCLE FATIGUE LIFE

In this paper, the high-cycle fatigue life characteristics are divided into the fatigue crack growth characteristics and the maximum defect size.

Versatile fatigue crack growth law (stress ratio $= -1$)

Under a small scale yielding condition, for example $\sigma_{\mathsf{a}} < 0.5\,\sigma_{\mathsf{S}}$ [15,16], the fatigue crack growth rate $d\,\ell/dN$, where ℓ is the total crack length on the specimen surface and N is a number of stress repetitions, is expressed as a the power of the stress intensity factor range, ΔK, as follows.

$$\frac{d\,\ell}{dN} = C(\Delta K)^{\mathsf{m}} \tag{1}$$

Here, σ_{a} is the stress amplitude, σ_{S} the yield stress, ℓ the total crack length on the specimen surface and N a number of cycle. On the other hand, under a large scale yielding condition, for example $\sigma_{\mathsf{a}} > 0.6\,\sigma_{\mathsf{S}}$ [15,16],

the following law of fatigue crack growth rate [16-19] in case of steels is satisfied for $R = -1$, where R is a stress ratio.

$$\frac{d\ell}{dN} = C_3 \left(\frac{\sigma_a}{\sigma_B} \right)^n \ell \tag{2}$$

Here, n and C_3 can be estimated from a database if the heat treatment and steel type are known.

Although there is a lot of fatigue data for steels, non ferrous materials have a few data. This is one obstacle to wide usage of new materials in mechanical engineering. Therefore in this paper, a fatigue crack growth rate law will be proposed from the fatigue crack growth mechanism and a few fatigue data.

The mode I type of fatigue crack growth is based on the successive plastic blunting and resharpening of the crack tip. Then at first, in a non-work-hardening materials, crack growth due to the plastic blunting under a monotonic stress σ is obtained from the dimensional analysis as follows.

$$\Delta a \propto \frac{\sigma_S}{E} f \left(\frac{\sigma}{\sigma_S} \right) a \tag{3}$$

Here, E is Young's modulus, a the half crack length, and Δa the increment of a. The crack growth due to plastic blunting is expressed concretely from CTOD with the Dugdale Model as follows.

$$\Delta a \propto \frac{8\sigma_S}{\pi E} \ln \left[\sec \left(\frac{\pi \sigma}{2\sigma_S} \right) \right] a \tag{4}$$

It is supposed that the crack behavior due to the cyclic stress strain relation or load history can be represented by σ_S for steels. Although the differences of these factors among the materials are very important in the fatigue life near the non-propagating crack limit, the differences may be the secondary factor in $N_f < 10^6$ region. Hence the differences are neglected in this report. Therefore considering Eqn.2, the fatigue crack growth law is presented as follows, by approximating $\ln[\sec(\pi/2 \times \sigma/\sigma_S)]$ with $(\sigma/\sigma_S)^n$.

$$\frac{d\ell}{dN} = C_4 \frac{\sigma_S}{E} \left(\frac{\sigma_a}{\sigma_S} \right)^n \ell \tag{5}$$

Figures 1 and 2 show C_4 and n values in Eqn.5 obtained from small crack growth data of steels [15], aluminum cast alloy [4,20], rolled aluminum alloy [18], brass [21] and titanum alloy [22]. In steels whose mechanical properties are dependent on the alloy element and heat treatment, n and C_4 in Eqn.5 should be functions of σ_S, however for simple use, n is taken to be constant; $n = 6$ in this paper.

$$\frac{d\ell}{dN} = C_5 \frac{\sigma_S}{E} \left(\frac{\sigma_a}{\sigma_S} \right)^6 \ell \tag{6}$$

Figure 3 shows C_5 values of Eqn.6 obtained from Figs.1 and 2. The following expression is a curve through the center of the data.

$$C_5 = \begin{cases} \frac{\sigma_S}{2500} & (\sigma_S \geq 300\text{MPa}) \\ \left(\frac{\sigma_S}{510} \right)^4 & (\sigma_S < 300\text{MPa}) \end{cases} \tag{7}$$

Even if materials are changed, most data lie between twice and half of Eqn.7 except for low carbon steels.

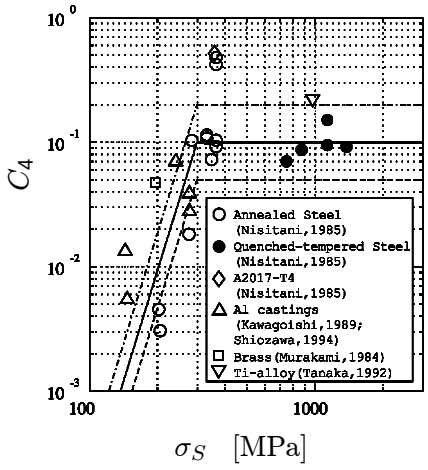

Figure.1: Relation between C_4 and σ_S

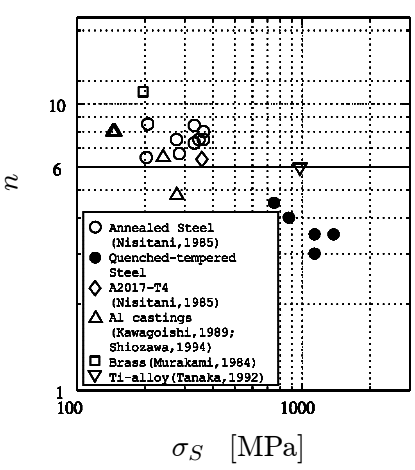

Figure.2: Relation between n and σ_S

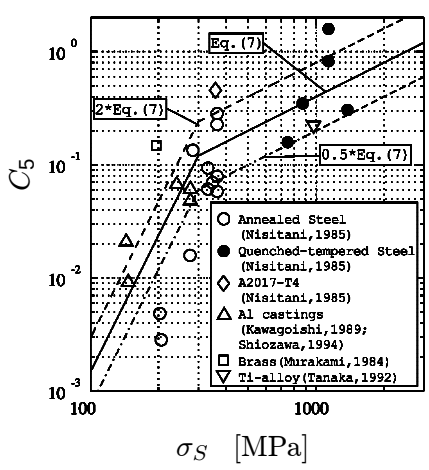

Figure.3: Relation between C_5 and σ_S

Particle size distribution

The authors [23] have proposed a method where a size distribution of particles in materials can be estimated from information on a cutting plane. The method is applied to eutectic Si, Fe compound and porosity in aluminum cast alloy. The size distribution of particles in materials can be assumed as follows.

$$M_{V0}(R_1) = \bar{N}_{V0} \exp\left\{-\left(\frac{R_1}{\lambda}\right)^{\nu}\right\} \tag{8}$$

Here, $M_{V0}(R_1)$ is the number of particles per unit volume whose radius, R, is larger than R_1, $\bar{N}_{V0}$ the total number of particles and λ and ν are the characteristic constants of the particle-size distribution.

According to the below-mentioned fatigue test, the fracture origins of the present materials were the surface defects. Therefore the characteristics of a particle cut by the specimen surface are examined from the size distribution of particles in the material.

The particle cut by the specimen surface is projected perpendicular to the first principal stress and the projected area is corrected on the basis of a fracture mechanics consideration. Then the corrected area is identified with $area_P$ as shown in Fig.4. The number of cut particles on the surface whose $\sqrt{area_P}$ is larger than $\sqrt{area_P}_1$, $M_{S0}(\sqrt{area_P}_1)$, can be expressed as

$$M_{S0}(\sqrt{area_P}_1) = \lambda \bar{N}_{V0} \int_0^1 \frac{t}{\sqrt{1-t^2}} \left\{\Gamma\left(1+\frac{1}{\nu}, \left(\frac{\sqrt{area_P}_1}{\lambda\sqrt{\theta^-}}\right)^{\nu}\right) + \Gamma\left(1+\frac{1}{\nu}, \left(\frac{\sqrt{area_P}_1}{\lambda\sqrt{\theta^+}}\right)^{\nu}\right)\right\} dt \tag{9}$$

$$\theta^+ = \frac{\pi}{2} + 2\sqrt{1-t^2}\,, \quad \theta^- = \arcsin(t) - t\sqrt{1-t^2} \tag{10}$$

Next, let us consider the probability distribution function of the maximum $\sqrt{area_P}$ value on area A, $\sqrt{area_P}_{max}$. The average number of particles whose $\sqrt{area_P}$ is larger than $\sqrt{area_P}_1$, is $A \cdot M_{S0}(\sqrt{area_P}_1)$. The probability that the $\sqrt{area_P}_{max}$ is smaller than $\sqrt{area_P}_1$, means the probability that there is no particle whose $\sqrt{area_P}$ is larger than $\sqrt{area_P}_1$. Using the Poisson's distribution, the probability is $\exp[-A \cdot M_{S0}(\sqrt{area_P}_1)]$. Therefore, the probability that the $\sqrt{area_P}_{max}$ is smaller than $\sqrt{area_P}_{max1}$, $F_{Smax}(\sqrt{area_P}_{max1})$, is expressed as follows.

$$F_{S\,max}(\sqrt{area_P}_{max_1}) = \exp[-M_S(\sqrt{area_P}_{max_1})] \tag{11}$$

Prediction of high-cycle fatigue life

Although the fatigue life consists of the fatigue crack nucleation life and growth life, it is supposed in this paper that the former life can be neglected and the main crack propagates from the maximum surface defect in the present materials. Moreover, although the scatter of the fatigue life consists of the scatter of the maximum defect size and the scatter of material properties in the crack propagation process, it is supposed in this paper that the former scatter can be considered as the main factor. That is; the fatigue life, N_f, is expressed from Eqn.6 as follows.

$$N_f = \frac{E}{C_5\,\sigma_S}\left(\frac{\sigma_S}{\sigma_a}\right)^n \ln\left\{\frac{d}{\frac{\pi}{8}\sqrt{area_P}_{max}}\right\} \tag{12}$$

Here, d is a diameter of a specimen. The scatter of the fatigue life depends on the scatter of $\sqrt{area_P}_{max}$ in Eqn.11 and it can be evaluated with Eqn.10.

Determination of C_5

With Eqn.7 for estimating C_5 in Eqn.6, the fatigue crack growth rate can be estimated within about $\pm 50\%$ error except for low strength steels. However, if the fatigue life data of the specimen with a small blind hole is measured under a certain stress amplitude, C_5 can be determined more accurately with Eqn.11. Moreover, if $d\ell/dN$ is measured under the stress amplitude, the validity of Eqn.6, where $n = 6$ is supposed, can be examined.

FATIGUE EXPERIMENT

A commertial JIS-AC4B alloy was used. The chemical compositions of the alloy is shown in Table 1. Figure 5 and Table 2 show the tensile properties and micro-Vickers hardness of α-Al after T6 treatment.

Fatigue tests were carried out on the plain specimen shown in Fig.6. For an examination of Section 2.4, a specimen with a small blind hole ($\phi 0.3 \times 0.15$mm) was used for an observation of fatigue crack growth. The specimen was machined, polished with fine emery paper, alumina(3μm) and diamond paste(1μm), and polished chemically. A Ono-type rotating bending fatigue machine, whose capacity was 15Nm and frequency was about 50Hz, was used for fatigue tests. The stress used in the analysis of experimental results is the nominal stress

at the minimum cross section.

Figure 7 shows S-N curves. The large scatter is particular in the present materials, compared with the usual materials. Therefore the measured $\sqrt{area_P}$ value of the fracture origin are added to the symbols in Fig.7. From Fig.7, it is found that the scatter of the fatigue life is small for the same $\sqrt{area_P}$ value of the fracture origin.

TABLE 1

CHEMICAL COMPOSITION (MASS %)

Si	Cu	Mg	Fe	Mn	Zn	Pb	Sr
6.79	2.93	0.17	0.59	0.49	0.17	0.05	138

Sr : ppm

TABLE 2

MECHANICAL PROPERTIES

σ_B	$\sigma_{0.2}$	δ	E	H_V of α(Al) 25g, 30 sec
349	292	1.50	74	124

σ_B :Ultimate Tensile Strength (MPa) $\sigma_{0.2}$:0.2% Proof Stress (MPa)
E: Young's Modules (GPa) δ:Elongation (%)
H_V :Micro Vickers Hardness (kgf/mm^2)

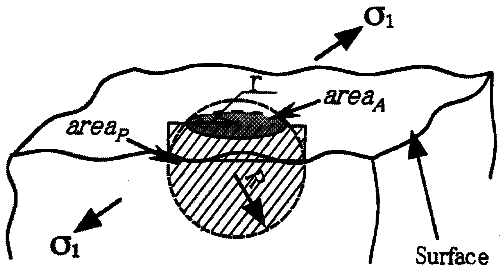

Figure.4: Shperoidal particle cut by surface

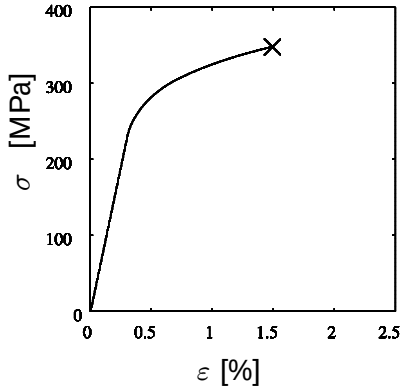

Figure.5: Stress-strain curve

PREDICTION RESULTS FOR ALUMINUM CAST ALLOY

Fatigue crack growth characteristics

Table 3 shows the C_5 values estimated from Eqn.7, using $\sigma_{0.2}$.

The fatigue test results for a specimen with a 0.3mm small hole under σ_a = 160 MPa are mentioned as follows. The C_5 values calculated from Eqn.11 under this stress level with the projected area of the drill hole, $\sqrt{area_P}_{max}$ = 180μm, are shown in Table 3. As the C_5 values from Eqns.7 and 11 agree with each other, it is confirmed that Eqn.7 as the first approximation is valid also in the present materials.

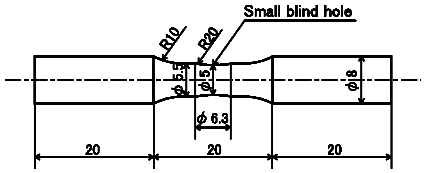

(a) plain specimen

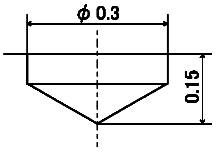

(b) small blind hole

Figure.6: Specimen configuration

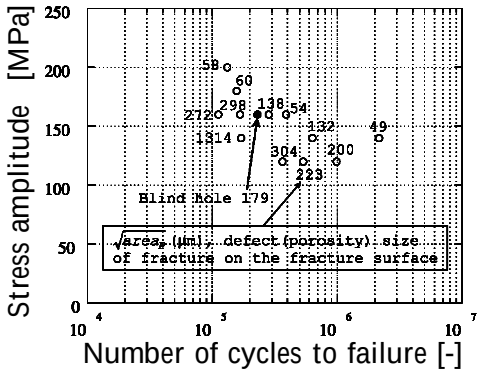

Figure.7: S-N curve

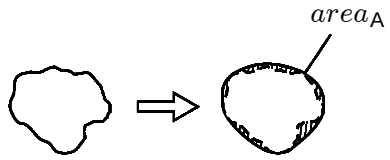

Figure.8: Definition of $area_A$

TABEL 3

C_5 VALUE OF PRESENT CAST ALLOY

Eqn.7	Eqn.11
0.11	0.14

Size distribution of particle

The actual particle or porosity is not a perfect sphere (for example, gas type and shrinkage type) and the cross-section of cut particle is not a perfect circle. Thus let's consider the measurement method of the cross-section radius, r. Surrounding an irregular cross-section with a smooth convex curve, the area is defined as $\sqrt{area_A}$

as shown in Fig.8. The r values are obtained from $\sqrt{area_A}$ values with the following relation.

$$r = \frac{\sqrt{area_A}}{\sqrt{\pi}} \tag{13}$$

Let us consider the radius of circle obtained from a cut sphere. The number of circles whose r is larger than r_1 per unit area, $M_{A0}(r_1)$, has a mutual relation with $M_{V0}(R_1)$ [23]. Especially if $M_{V0}(R_1)$ is supposed with Eqn.8, $M_{A0}(r_1)$ is expressed as follows.

$$M_{A0}(r_1) = \sqrt{\frac{2\pi}{\nu}} \lambda \left(\frac{r_1}{\lambda}\right)^{1-\frac{\nu}{2}} \bar{N}_{V0} \exp\left[-\left(\frac{r_1}{\lambda}\right)^{\nu}\right] \tag{14}$$

Figure 9 shows the experimental data for $M_{A0}(\sqrt{area_A})$ of eutectic Si, Fe compound and porosity of each material. The $\bar{N}_{V0}, \lambda$ and ν values of Eqn.8 were determined after drawing the curve of Eqn.8, which is an optimum fit to the data. Figures 12 and 13 show $M_{V0}(R)$ and $M_{S0}(\sqrt{area_P})$, respectively.

When the inspection area, A, is taken as the area whose stress is $(1 \sim 0.9)\sigma_{max}$ on the specimen surface, A=60 mm^2 in case of the present specimen. Figure 17 shows $F_{Smax}(\sqrt{area_P}_{max})$ on the present area. It is possible that the surface porosity is the fracture origin in AC4B-T6.

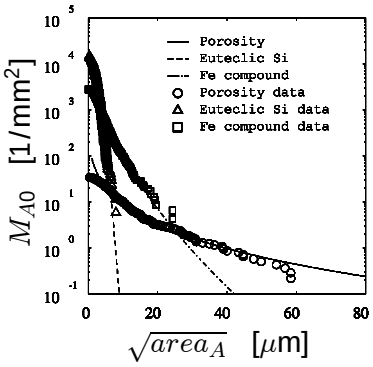

Figure.9: $M_{A0}(\sqrt{area_A})$

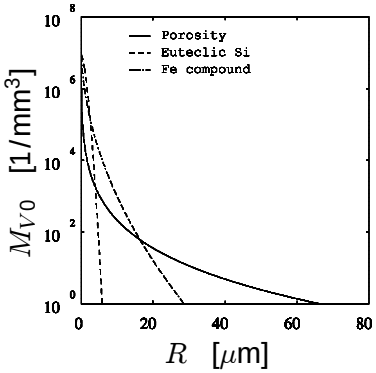

Figure.10: $M_{V0}(\sqrt{area_R})$

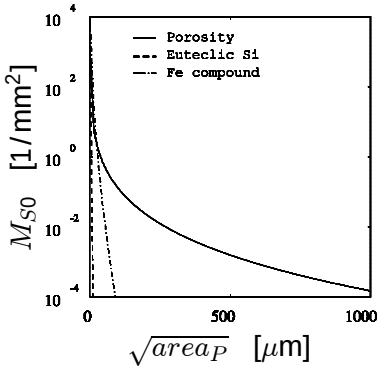

Figure.11: $M_{S0}(\sqrt{area_P})$

Comparison between predicted and experimental fatigue life

A cumulative distribution of $\sqrt{area_P}$ values observed on the fracture surface was obtained from Fig.7 using the mean rank method. Figure 13 shows both the cumulative distribution of porosity. As results of Fig.13, it is found that the estimation method for the probability distribution of $\sqrt{area_P}_{max}$ is valid and the maximum value of $\sqrt{area_P}$ of cut porosity with the specimen surface controls the fatigue strength of the present aluminum cast alloy.

Therefore the fatigue life reliability of the present specimen shown in Fig.5 can be estimated by using Eqn.10 which expresses the statistical characteristics of $\sqrt{area_P}_{max}$ of porosity, and Eqn.11 which expresses the fatigue life due to fatigue crack growth. Namely, the fatigue life reliability such that the fatigue life is greater than N_{f1}, F_{N_f}, is

$$F_{N_f}(N_{f1}) = F_{Smax}(\sqrt{area_P}_{max1}) \tag{15}$$

$$N_{f1} = \frac{E}{C_5 \sigma_S}\left(\frac{\sigma_S}{\sigma_a}\right)^6 \ln\left[\frac{d}{\frac{\pi}{8}\sqrt{area_P}_{max}}\right] \tag{16}$$

Figure 14 shows the predicted results from meso-level data and experimental data.

As a result, the following is found. Although the fatigue life characteristic of AC4B cannot be evaluated quantitatively from the macro-scale fatigue characteristic of Fig.7, the characteristics can be evaluated quantitatively from the meso-scale material characteristics with Table 3, and Figs.12 and 13.

CONCLUSION

1. The prediction method for the data scatter of high-cycle fatigue life has been proposed with microscope observations for cross-section size distribution of particles cut by a cutting plane.
2. The predicted results have been confirmed for aluminum cast alloy.

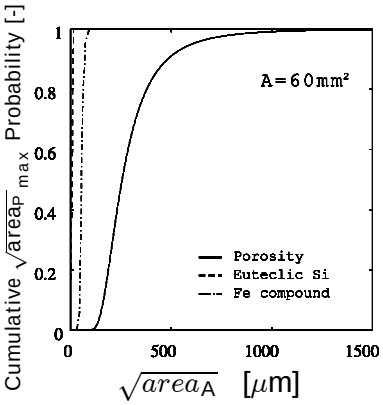

Figure.12: $F_{Smax}(\sqrt{area_P}_{max})$

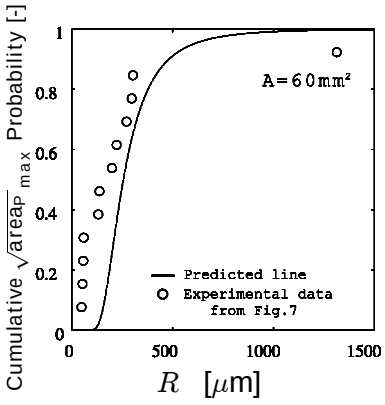

Figure.13: Cumulative $\sqrt{area_P}_{max}$

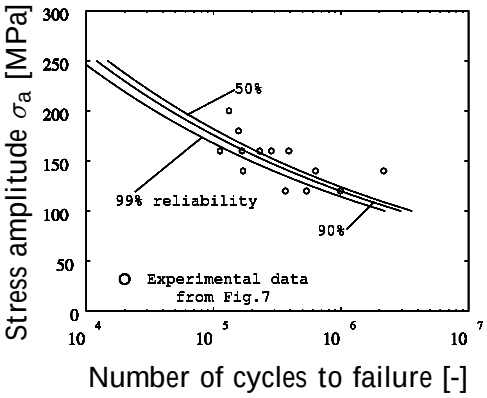

Figure.14: Estimated S-N reliability

REFERENCE

[1] Kobayashi,T., Niinomi,M. and Ikeda,K.,(1987). International Journal of Fracture, 37-12, pp.824-830.
[2] Egashira,H., Hirota,I., Kobayashi,T. and Sakai,S.,(1989). Journal of Japan Institute of Light Metals, 39-12, pp.878-885.
[3] Egashira,H., Hirota,I., Kobayashi,T. and Sakai,S.,(1989). Journal of Japan Institute of Light Metals, 39-12, pp.886-892.
[4] Shiozawa,K.,Nisino,S.,Higashida,Y. and Sun,S.M.,(1994). Jounal of Japan Institute of Light Metals, 38-4, pp.202-207.
[5] Lee,F.T., Major,J.F. and Samuel,F.H.,(1995). Metallurgical and Materials Trans. A., 26A, pp.1553-1570.
[6] Kobayashi,T., Ito,T., Kim,H. and Kitaoka,S.,(1996). Journal of Japan Institute of Light Metals, 46-9, pp.437-443.
[7] Kumai,S., Hu,J., Higo,Y. and Ninomura,S.,(1995). Journal of Japan Institute of Light Metals, 45-4, pp.198-203.
[8] Gobrecht,B.,(1976). Journal of Japan Institute of Light Metals, 39-12, pp.886-892.
[9] Couture,A.,(1981). AFS International Cast Metals Journal, 6-4, pp.9-17.
[10] Shimizu,Y. and Awano,Y., Nakamura,M.,(1988). Jounal of Japan Institute of Light Metals, 38-4, pp.202-207.
[11] Kato,E. and Murakawa,S.,(1994). Journal of Japan Foundry Engineering Society, 66-1, pp.10-14.
[12] Iwahori,H., Takamiya,H., Yonekura,H., Yamamoto,Y. and Nakamura,Y.,(1988). J. of Japan Foundry Engng. Soc., 60-9, pp.590-595.
[13] Sigworth,G.K.,(1987). Modern Casting, July, pp.23-25.
[14] Kang,H.G., Miyahara,H. and Ogi,K.,(1997). Journal of Japan Foundry Engineering Society, 69-5, pp.383-390.
[15] Nisitani,H.,(1981). Mechanics of Fatigue, AMD 47,ASME, pp.151-166..
[16] Nisitani,H., Kawagoishi,N. and Goto,M.,(1994). In Handbook of fatigue crack propagation in metallic structures (Edited by Carpinteri,A.),Elsevier,Amsterdam, pp.733-778.
[17] Nisitani,H. and Goto,M.,(1985). Transaction of Japanese Society of Mechanical Engineers, A51-462, pp.332-341.
[18] Nisitani,H., Kawagoishi,N. and Wakahara,M.,(1985). Transaction of Japanese Society of Mechanical Engineers, A51-464, pp.1017-1025.
[19] Goto,M. and Nisitani,H.,(1994). Fatigue and Fracture of Engng. Mater. Struct., 17, pp.171-185.
[20] Kawagoishi,N., Nisitani,H. and Tsuno,T.,(1989). Transaction of Japanese Society of Mechanical Engineers, A55-516, pp.1733-1739.
[21] Murakami,Y., Makabe,C. and Nisitani,H.(1984). Transaction of Japanese Society of Mechanical Engineers, A50-459, pp.1828-1837.
[22] Tanaka,S.,Nisitani,H.,Fujisaki,W.,Teranisi,T.,Honda,M.,(1992). Journal of Japanese Society of Material Science, 41-469, pp.1485-1491.
[23] Hashimoto,A., Miyazaki,T., Kang,H.G., Noguchi,H. and Ogi,K.,(2000). Jounal of Testing and Evaluation, 28-9, pp.367-377.